On the non-linear spectroscopy including saturated absorption and four-wave mixing in two and multi-level atoms: a computational study

M Patel[1], G De Jager[2], Z Nkosi[3], A Wyngaard[4] and K Govender[5,6]

[1,3,4,5] Department of Electrical, Electronic and Computer Engineering, Cape Peninsula University of Technology, Symphony Way, Bellville, Cape Town, 7535, South Africa

[2] Department of Electrical Engineering, University of Cape Town, Rondebosch, 7701, South Africa

[6] School of Chemistry and Physics, University of KwaZulu-Natal, South Africa

E-mail: [1]210230177@mycput.ac.za

Abstract. In this paper we report on the study of two and multi-level atoms interacting with multiple laser beams. The semi-classical approach is used to describe the system in which the atoms are treated quantum mechanically via the density matrix operator, while the laser beams are treated classically using Maxwells equations. We present results of a two level atom interacting with single and multiple laser beams and demonstrate Rabi oscillations between the levels. The effects of laser modulation on the dynamics of the atom (atomic populations and coherences) are examined by solving the optical Bloch equations. Plots of the density matrix elements as a function of time are presented for various parameters such as laser intensity, detuning, modulation etc. In addition, phase-space plots and Fourier analysis of the density matrix elements are provided. The atomic polarization, estimated from the coherence terms of the density matrix elements, is used in the numerical solution of Maxwells equations to determine the behaviour of the laser beams as they propagate through the atomic ensemble. The effects of saturation and hole-burning are demonstrated in the case of two counter propagating beams with one being a strong beam and the other being very weak. The above work is extended to include four-wave mixing in four level atoms in a diamond configuration. Two co-propagating beams of different wavelengths drive the atoms from a ground state $|1\rangle$ to an excited state $|3\rangle$ via an intermediate state $|2\rangle$. The atoms then move back to the ground state via another intermediate state $|4\rangle$, resulting in the generation of two additional correlated photon beams. The characteristics of these additional photons are studied.

1. Background

Quantum properties of light, besides being a subject of fundamental interest, is being used in emerging technologies such as quantum cryptography and quantum computing. There are a variety of ways of generating quantum light, however here we aim to investigate the generation and properties of quantum light using non-linear processes in cold atoms. We investigate the generation and subsequent properties of coherent light by means of four-wave mixing in an ensemble of cold rubidium atoms.

The motivation for this study is the fact that there is growing evidence that the next generation of computing and communication is going to be quantum based, i.e. these systems

operate using the principles of quantum physics. These systems will operate using fundamentally new principles that involve light-atom interactions on a single photon level and ambitious schemes such as quantum teleportation. For long distance communications these schemes have to be implemented using entangled photons.

Entangled photons produced by four-wave mixing in a cold atomic ensemble have been shown to have desirable features. These photons have a narrow bandwidth, which is determined by the dispersion of the vapour and can be narrow enough to match the absorption profile of the atoms. These biphoton sources have properties such as long coherence time, long coherence length, high spectral brightness and high conversion efficiency. There have been a number of books and papers describing laser-atom interactions (e.g. see [1, 2, 3, 4, 5, 6]), and entangled photon pair generation using four-wave mixing in rubidium atomic ensembles [7, 8, 9, 10, 11].

We report on the computational study of the interaction between laser beams and, two and multi-level atoms. We use a semi-classical approach in which the dynamics of the atoms (described by the density matrix elements) are governed by the Liouville-von Neumann equation,

$$\frac{\partial \hat{\rho}}{\partial t} = -\frac{\imath}{\hbar}\left[\hat{H}, \hat{\rho}\right] + L_{damp}(\hat{\rho}) \tag{1}$$

while the laser beam is described by the wave equation derived from Maxwell's equations. The Hamiltonian of the total system is $\hat{H} = \hat{H}_0 + \hat{H}_I$, where $\hat{H}_0$ is the unperturbed Hamiltonian and $\hat{H}_I$ is the interaction term. The effects of dissipation are contained in $L_{damp}(\hat{\rho})$. We first discuss a two level atom interacting with a single laser beam and examine the dynamics of the population and coherence terms of the density matrix elements. Thereafter we examine the behaviour of the laser beam as it propagates first in two level atoms and later in multi-level atoms.

The overview of the paper is as follows: Section 2 describes the interaction of a two level atom with a single laser beam. Results showing the effects of a uniform and modulated laser beam are given. Saturated absorption spectroscopy is discussed in Section 3. Results are given for various parameters followed by a discussion on non-linear mixing and entangled photon generation.

2. Laser-atom interactions in two level atoms

Consider an atom having two energy states represented by a ground state $|1\rangle$ having energy E_1 and an excited state $|2\rangle$ having energy E_2. Assume these states are separated in frequency by ω_0. Now let a laser beam with an electric field

$$\vec{E}(t) = \vec{E}_0 \cos \omega t$$

interact with a sample of these atoms, which are stationary. In the above, $\vec{E_0}$ is the amplitude of the electric field of the laser beam, $\cos \omega t$ represents the time variation of the electric field of the laser beam and ω is the laser frequency.

Then the following Hamiltonian describes the interaction:

$$\hat{H}_I = -\hat{\mu} \cdot \vec{E_0} \cos \omega t \tag{2}$$

where $-\hat{\mu}$ represents the dipole moment operator of the atom. The Liouville-von Neumann equation makes use of $\hat{H}_I$ to describe the time evolution of the density matrix elements of the system $\hat{\rho} = \sum_i P_i |i\rangle\langle i|$, where P_i is the probability of the atom being in state $|i\rangle$. It is used to derive the optical Bloch equations [3](below) for a two level atom:

$$\frac{\partial \rho_{11}}{\partial t} = \frac{\imath}{2}\Omega(\rho_{12} - \rho_{21}) + 2\gamma_{sp}\rho_{22} \tag{3}$$

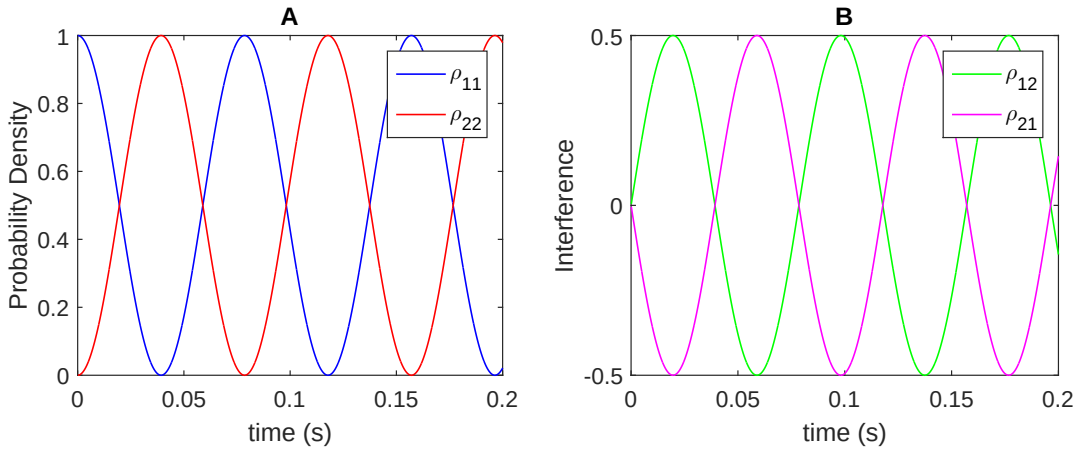

Figure 1. Rabi oscillations of a two level atom interacting with a uniform laser beam. Plots are: (**A**) - probability density and (**B**) - interference terms.

$$\frac{\partial \rho_{12}}{\partial t} = \frac{\imath}{2}\Omega(\rho_{11} - \rho_{22}) + \Big[\imath(\omega_0 - \omega) - \gamma_{sp}\Big]\rho_{12} \tag{4}$$

$$\frac{\partial \rho_{21}}{\partial t} = -\frac{\imath}{2}\Omega(\rho_{11} - \rho_{22}) + \Big[-\imath(\omega_0 - \omega) - \gamma_{sp}\Big]\rho_{21} \tag{5}$$

$$\frac{\partial \rho_{22}}{\partial t} = -\frac{\imath}{2}\Omega(\rho_{12} - \rho_{21}) - 2\gamma_{sp}\rho_{22} \tag{6}$$

where $\Omega = \langle\hat{\mu}\rangle E_0/\hbar$ is known as the Rabi frequency and γ_{sp} represents a decay/de-coherence coefficient. ρ_{11} and ρ_{22} tell us the probability of the atom being in the ground and excited states respectively. ρ_{12} and ρ_{21} are the interference terms of the atom indicative of superposition. We solve the above numerically first for a uniform laser beam and then for a frequency modulated laser beam.

2.1. Results

Results of the numerical solution of Equations (3-6) are given in Figures 1-3 which correspond to a uniform laser beam while Figures 4-6 deal with a frequency modulated laser beam. In all the plots labelled **A**, the blue curve represents ρ_{11} and the red curve ρ_{22}. The green curve represents ρ_{12} and the magenta curve ρ_{21} in Figures 1-3**B**. The laser is switched on at time $t = 0\ s$ with $\rho_{11} = 100\%$ and $\rho_{22} = 0\%$. Rabi oscillations are demonstrated in Figure 1 where $\omega_0 - \omega = 0$. When $\rho_{11}, \rho_{22} = 50\%$ maximum superposition is achieved. In Figure 2 the effects of laser detuning can be seen i.e. $\omega_0 - \omega \neq 0$. The interference between Ψ_1 and Ψ_2 is decreased, where Ψ_i is the wave function corresponding to level i. When a small dissipation is introduced in the form of γ_{sp}, the effects can be seen in Figure 3. The interference between Ψ_1 and Ψ_2 decays to the point where the probability of superposition is close to 0%.

Laser beam modulation is introduced by adding a sinusoidal variation to the existing laser frequency

$$\omega_{laser} = \omega + D\sin(2\pi\omega_m t) \tag{7}$$

where ω is a fixed value, ω_m is the modulation frequency and D represents the magnitude of variation in ω_{laser}. The effects of laser modulation can be seen in Figures 4-6. In Figure 4 the modulation frequency is chosen to be greater than the Rabi frequency $\Omega = 12.73\ s^{-1}$. From Figure 4**A** the time series shows a clear pattern for the modulation. Figure 4**B** is the phase space plot indicating that the atom returns to the ground state after each oscillation. The

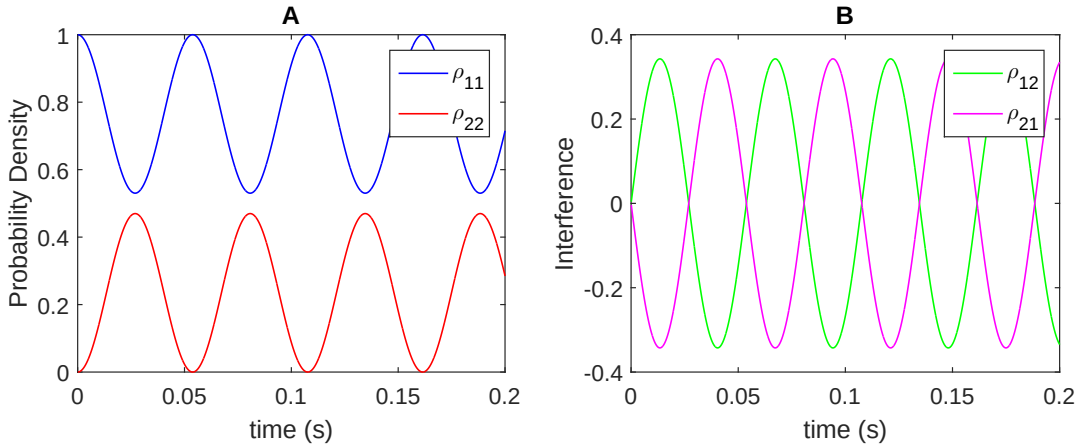

Figure 2. A two level atom interacting with a uniform laser beam that is detuned. Plots are: (**A**) - probability density and (**B**) - interference terms.

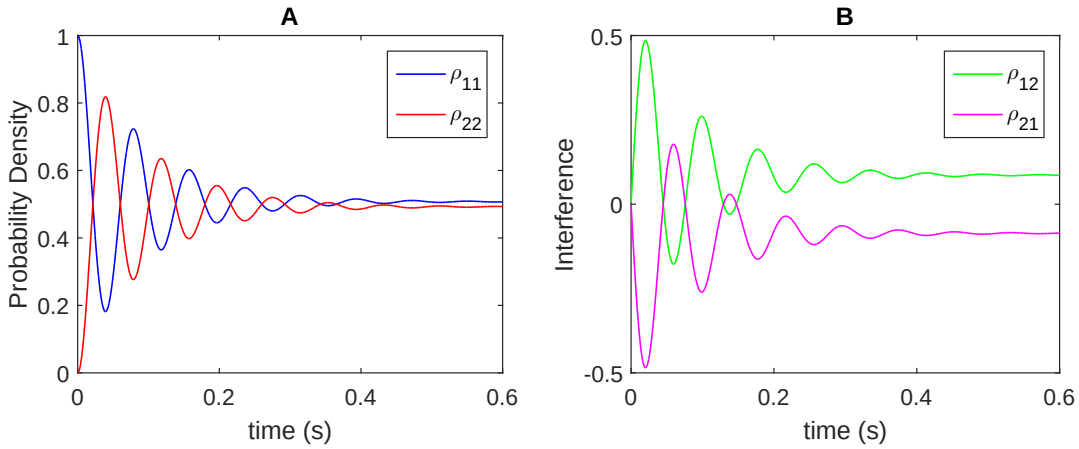

Figure 3. A two level atom interacting with a uniform laser beam where the dissipation coefficient is non-zero. Plots are: (**A**) - probability density and (**B**) - interference terms.

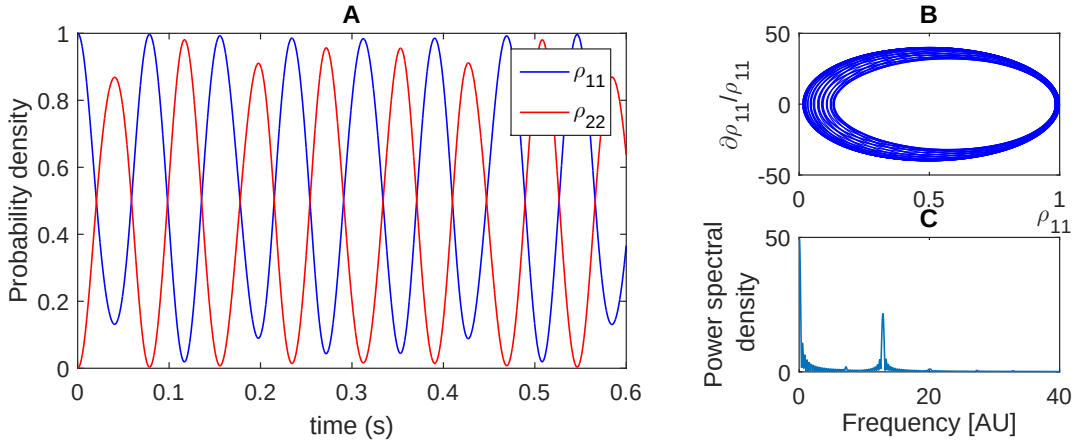

Figure 4. A two level atom interacting with a modulated laser beam where the modulation frequency is greater than the Rabi frequency. Plots are: (**A**) - probability density; (**B**) - phase space; and (**C**) - power spectral density. NB: In (**A**) only a few cycles are shown.

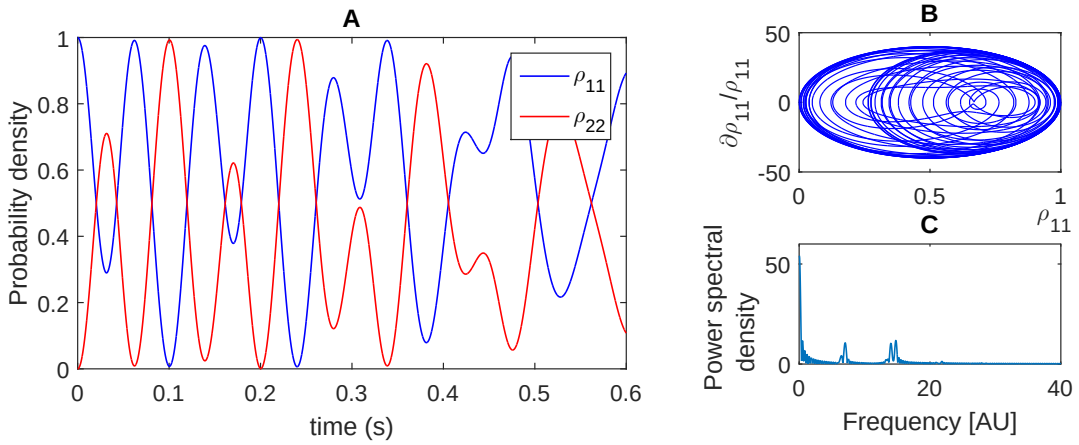

Figure 5. A two level atom interacting with a modulated laser beam where the modulation frequency is less than the Rabi frequency. Plots are: (**A**) - probability density; (**B**) - phase space; and (**C**) - power spectral density. NB: In (**A**) only a few cycles are shown.

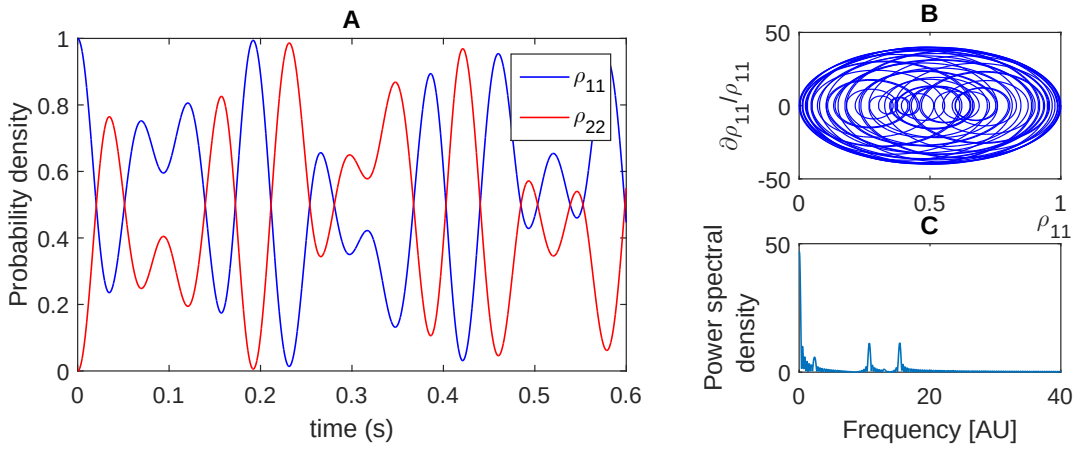

Figure 6. A two level atom interacting with a modulated laser beam where the modulation frequency is similar to the Rabi frequency. Plots are: (**A**) - probability density; (**B**) - phase space; and (**C**) - power spectral density. NB: In (**A**) only a few cycles are shown.

power spectral density, Figure 4**C**, shows a peak (around $13\,s^{-1}$) indicating the most prominent frequency besides the average value at the origin. A frequency that is less than the Rabi frequency is used to generate Figure 5. The time series, Figure 5**A**, depicts an irregular pattern for the modulation. The phase space plot, Figure 5**B** confirms this by indicating that the atom does not always transition to an expected state. Multiple peaks of similar amplitude are seen in the power spectral density, Figure 5**C** where the first peak is located at the modulated frequency ω_m and the second is located at $2\omega_m$. Finally, the modulation frequency is chosen to be similar to the Rabi frequency and is depicted in Figure 6. From Figure 6**A** it can once again be seen that an irregular pattern occurs which is also confirmed by the phase space plot, Figure 6**B**. In Figure 6**C** the power spectral density shows two peaks of the same amplitude located on either side of the Rabi frequency ($12.73\,s^{-1}$). These results show that the atom displays chaotic behaviour. Similar results have been seen by Pisipati et al [12].

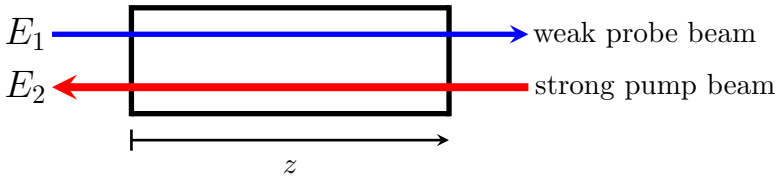

Figure 7. Basic arrangement for saturated absorption spectroscopy.

3. Saturated absorption spectroscopy

Next we look at the effect atoms have on the propagation of the laser beams which is done by making use of the basic arrangement depicted in Figure 7. Counter-propagating beams, E_1 and E_2, having the same frequency but different electric fields are passed through a gaseous sample after which the probe beam intensity is measured. The total electric field (in the laboratory frame) is given by

$$\vec{E} = (\vec{E}_1 e^{\imath kz} + \vec{E}_2 e^{-\imath kz}) e^{-\imath\omega t} \tag{8}$$

Assuming all the waves propagate in the z-direction we substitute Equation (8) in the wave equation

$$\nabla^2 \vec{E} - \frac{1}{c^2}\frac{\partial^2}{\partial t^2}\left(\vec{E} + \frac{\vec{P}}{\varepsilon_0}\right) = 0 \tag{9}$$

where $\vec{P}$ represents the polarization due to the applied electric filed, and we make use of the slowly varying approximation to obtain the following equation for the amplitude E_1 [2]

$$\frac{\partial E_1(z)}{\partial z} = \imath\frac{\omega}{2\epsilon_0 nc} P \tag{10}$$

Equation (10) is used to predict the behaviour of the electric field as it propagates through the sample where P is the total polarization given by

$$P = \int dv \underbrace{\left[\frac{1}{\sqrt{\pi}v_0} e^{-\frac{v^2}{v_0^2}}\right]}_{\mathbf{a}} \underbrace{\left[1 - \frac{\Omega_2^2}{\Gamma_{sp}} \frac{\gamma}{(\omega_0-\omega_2)^2 + \gamma^2 + \Omega_2^2 \frac{\gamma}{\Gamma_{sp}}}\right]}_{\mathbf{b}} \ldots$$
$$\ldots \underbrace{\left[\frac{N}{V}\frac{|\mu_{12}|^2}{2\hbar} \frac{\imath\gamma + (\omega_0-\omega_1)}{(\omega_0-\omega_1)^2 + \gamma^2 + \Omega_1^2 \frac{\gamma}{\Gamma_{sp}}} E_1 e^{-\imath\omega t}\right]}_{\mathbf{c}} \tag{11}$$

where μ_{12} is the matrix element of the dipole moment and Ω_1 and Ω_2 are the Rabi frequencies due to the electric fields E_1 and E_2 respectively. The velocity of the atoms is denoted by v and v_0 is the rms velocity, N/V is the density of atoms, Γ_{sp} is the decay of the population of the upper level and γ is the decay of the coherence [2, 13]. Equation (11) is a sum of all the polarizations due to the atoms and takes into account the various thermal velocities as well. When doing this, the atoms see the laser frequency as being Doppler shifted, this results in a broadening of the absorption profile. The square bracket labelled **a** in Equation (11) caters for the atomic velocity distribution and has a Gaussian profile. The fraction of atoms that part-take in the polarization is given by the square bracket labelled **b** in Equation (11) and is unity for all ω except close to $\omega_2 = \omega_0$ where ω_2 is the frequency of the pump beam as seen by the atoms moving with velocity v. At and close to $\omega_2 = \omega_0$ a dip indicates a reduction in the number of atoms in the ground state, this effect is referred to as hole burning. The square bracket labelled

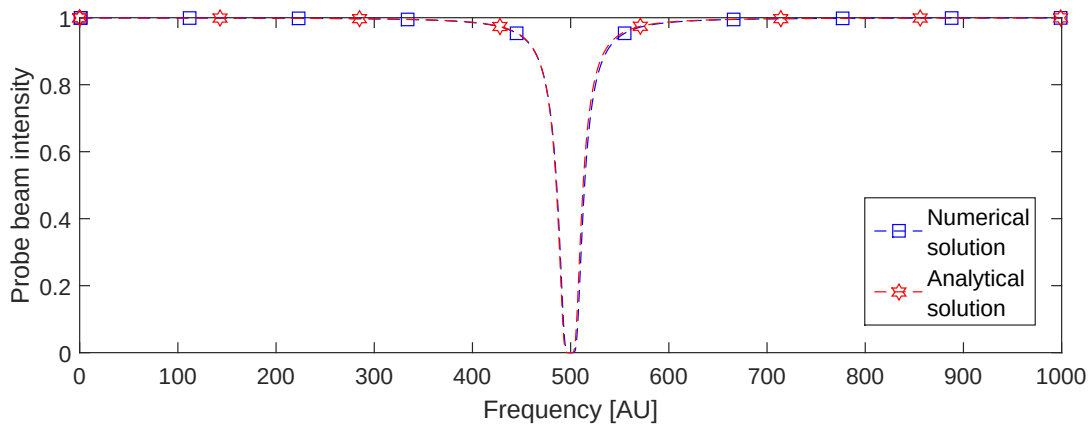

Figure 8. A comparison between the analytical and numerical solution of the probe beam intensity for frequencies above and below resonance for a particular spatial point in the sample.

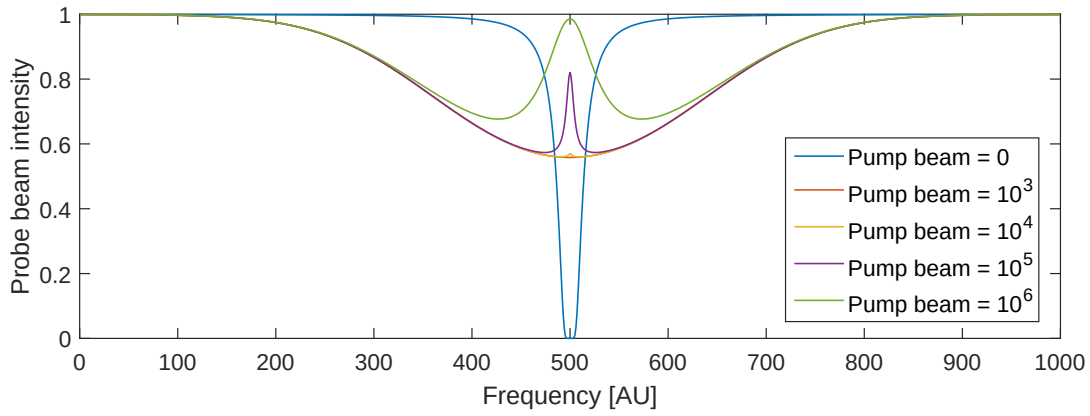

Figure 9. The probe beam intensity with increasing values of pump beam field, E_2.

c in Equation (11) is the term representing the polarization due to the probe beam which has a frequency ω_1. These terms are derived theoretically from the optical Bloch equations [2, 13].

3.1. Results

First we analyse the system with all atoms having zero velocity and interacting with the probe beam. Using Equation (10) results in the analytical solution for the intensity of the probe beam

$$|I| = I_0 e^{-2\alpha z} \tag{12}$$

where

$$\alpha = \frac{\omega}{2\epsilon_0 nc}\frac{N}{V}\frac{|\mu_{12}|^2}{2\hbar}\frac{\gamma}{(\omega_0-\omega)^2+\gamma^2} \tag{13}$$

This demonstrates absorption and is depicted by Figure 8 which shows a comparison between the analytical solution, where I is calculated using Equation (12), and the numerical solution, where I is obtained by solving Equation (10). Figure 8 shows satisfactory agreement between the two solutions.

The ground and excited state populations of the atoms are altered by the pump beam. The electric field of the pump beam is made strong enough to saturate the sample, therefore changing the measured absorption. Figure 9 demonstrates this change where the blue curve depicts the probe beam intensity for atoms having zero velocity and the pump beam electric field being zero. The thermal velocity of the atoms are then taken into account and the pump beam electric field is gradually increased. From Figure 9 the orange, yellow, purple and green curves depict the effects the pump beam has on the sample. It can be seen that when the thermal velocities are taken into account the absorption profile is broadened whilst the absorption at and close to resonance is decreased (showing the true Lorentzian profile) resulting in the intensity to increase. We assume in the above that the pump beam is strong enough so that it remains unchanged as it propagates through the sample.

4. Four-wave Mixing

We now examine a non-linear mixing process using a diamond energy level structure to simulate four-wave mixing in rubidium gas. We examine four-wave mixing using the energy level structure shown in Figure 10. These states could represent those of ^{87}Rb as shown in brackets.

E_1 to E_4 are the corresponding energies of each level, ω_1 and ω_2 are frequencies of two pump

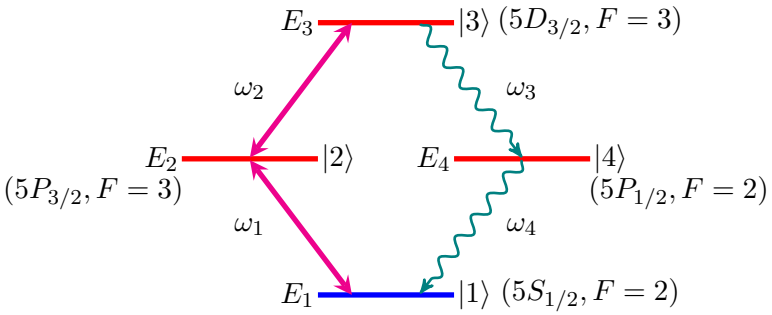

Figure 10. Four-wave mixing geometry.

lasers and ω_3 and ω_4 are frequencies of two internally generated photons.

We will assume that the pump laser beams are strong enough that they do not deplete as they propagate through the atomic ensemble. We will also assume that all photons propagate in the positive z-direction. The atomic levels are assumed to be such that the photons of frequency ω_1, ω_2, ω_3 and ω_4 couple only transitions between $|1\rangle \leftrightarrow |2\rangle$, $|2\rangle \leftrightarrow |3\rangle$, $|3\rangle \leftrightarrow |4\rangle$ and $|4\rangle \leftrightarrow |1\rangle$, respectively, that is they are very much detuned compared to the other transitions. The total electric field is then

$$E = \sum_{i=1}^{4} \left(\tilde{E}_i e^{-\imath\omega_i t} + c.c. \right) \tag{14}$$

where

$$\tilde{E}_i = E_i(z) e^{\imath k_i z} \tag{15}$$

The electric field amplitudes E_i should not be confused with the energy levels. The behaviour of the electric field E_3 and E_4 due to the frequencies ω_3 and ω_4 are described by Maxwell's equations:

$$\frac{\partial}{\partial z} E_3(z) = \imath \frac{\omega_3}{2\epsilon c} \frac{N}{V} \mu_{34} \rho_{34}^{(3)} \tag{16}$$

$$\frac{\partial}{\partial z} E_4(z) = \imath \frac{\omega_4}{2\epsilon c} \frac{N}{V} \mu_{41} \rho_{41}^{(3)} \tag{17}$$

where $\rho_{ij}^{(3)}$ are the third order density matrix elements and are obtained from the master equation as described below.

The total Hamiltonian is

$$H = H_0 + H_I \tag{18}$$

where $H_I = -\hat{\mu} \cdot E$ and $-\hat{\mu}$ is the dipole moment of the atom. We will use the following as a basis:

$$|\Psi_1\rangle = e^{-\imath E_1 t/\hbar}|1\rangle \tag{19}$$
$$|\Psi_2\rangle = e^{-\imath E_2 t/\hbar}|2\rangle \tag{20}$$
$$|\Psi_3\rangle = e^{-\imath E_3 t/\hbar}|3\rangle \tag{21}$$
$$|\Psi_4\rangle = e^{-\imath E_4 t/\hbar}|4\rangle \tag{22}$$

In the above basis

$$H_0 = \begin{pmatrix} E_1 & 0 & 0 & 0 \\ 0 & E_2 & 0 & 0 \\ 0 & 0 & E_3 & 0 \\ 0 & 0 & 0 & E_4 \end{pmatrix} \tag{23}$$

and $H_I' = e^{-\imath H_0 t/\hbar}\, H_I\, e^{\imath H_0 t/\hbar}$ becomes

$$E \begin{pmatrix} 0 & -\mu_{12}e^{\imath\omega_{12}t} & -\mu_{13}e^{\imath\omega_{13}t} & -\mu_{14}e^{\imath\omega_{14}t} \\ -\mu_{21}e^{\imath\omega_{21}t} & 0 & -\mu_{23}e^{\imath\omega_{23}t} & 0 \\ -\mu_{31}e^{\imath\omega_{31}t} & -\mu_{32}e^{\imath\omega_{32}t} & 0 & -\mu_{34}e^{\imath\omega_{34}t} \\ -\mu_{41}e^{\imath\omega_{41}t} & 0 & -\mu_{43}e^{\imath\omega_{43}t} & 0 \end{pmatrix} \tag{24}$$

where $\omega_{ij} = (E_i - E_j)/\hbar$ and $\mu_{ij} = \langle i|\hat{\mu}|j\rangle$. Then the Liouville-von Neumann equation (also known as the master equation) that we solve is

$$\dot{\rho} = -\frac{\imath}{\hbar}\left[H_I', \rho\right] + relaxation\, terms \tag{25}$$

Using perturbation theory we let

$$\rho = \rho^{(0)} + \lambda\rho^{(1)} + \lambda^2\rho^{(2)} + ... \tag{26}$$

We also expand each $\rho^{(i)}$ in frequency as well and also we replace H_I' by $\lambda H_I'$. We assume at zero order $\rho_{11}^{(0)} = 1$ with all other terms being zero, i.e.

$$\rho^{(0)} = \begin{pmatrix} 1 & 0 & 0 & 0 \\ 0 & 0 & 0 & 0 \\ 0 & 0 & 0 & 0 \\ 0 & 0 & 0 & 0 \end{pmatrix} \tag{27}$$

In the rotating wave approximation, the first order solutions we find that are non-zero are

$$\tilde{\rho}_{21}^{(1)} \simeq \frac{1}{\hbar}\mu_{21}\frac{E_1}{\Delta_{21} - \imath\Gamma_{21}}e^{-\imath\omega_1 t} \tag{28}$$

and

$$\tilde{\rho}_{41}^{(1)} \simeq \frac{1}{\hbar}\mu_{41}\frac{E_4}{\Delta_{41} - \imath\Gamma_{41}}e^{-\imath\omega_4 t} \tag{29}$$

plus their complex conjugates where $\tilde{\rho}_{ij}^{(1)} = \rho_{ij}^{(1)} e^{-\imath\omega_{ij}t}$. All the other terms are zero. The third order terms that are important for solving Maxwell's equation for the ω_3 and ω_4 terms are

$$\begin{aligned}\tilde{\rho}_{34}^{(3)} \simeq \frac{1}{\Delta_{34} - \imath\Gamma_{34}} \Bigg[& \frac{2}{\gamma_{41}} \frac{|\mu_{14}|^2 \mu_{34}}{\hbar^3} \frac{|E_4|^2 E_3 \Gamma_{41}}{\Delta_{41}^2 + \Gamma_{41}^2} + \frac{\mu_{14}\mu_{32}\mu_{21}}{\hbar^3} \frac{E_1 E_2 E_4^*}{(\Delta_{42} + \imath\Gamma_{41})} \Bigg(\frac{1}{(\Delta_{21} - \imath\Gamma_{21})} \\ & - \frac{1}{(\Delta_{41} + \imath\Gamma_{41})} \Bigg) - \frac{\mu_{14}\mu_{32}\mu_{21}}{\hbar^3} \frac{E_1 E_2 E_4}{(\Delta_{31} - \imath\Gamma_{31})(\Delta_{21} - \imath\Gamma_{21})} \\ & - \frac{\mu_{14}\mu_{34}\mu_{41}}{\hbar^2} \frac{E_3 |E_4|^2}{(\Delta_{31} - \imath\Gamma_{31})(\Delta_{41} - \imath\Gamma_{41})} \Bigg] e^{-\imath\omega_3 t}\end{aligned} \tag{30}$$

and

$$\begin{aligned}\tilde{\rho}_{41}^{(3)} \simeq \frac{1}{\Delta_{41} - \imath\Gamma_{41}} \Bigg[& -\frac{2}{\gamma_{21}} \frac{|\mu_{12}|^2 \mu_{41}}{\hbar^3} \frac{|E_1|^2 E_4 \Gamma_{21}}{\Delta_{21}^2 + \Gamma_{21}^2} - \frac{4}{\gamma_{41}} \frac{|\mu_{14}|^2 \mu_{41}}{\hbar^3} \frac{|E_4|^2 E_4 \Gamma_{41}}{(\Delta_{41}^2 + \imath\Gamma_{41}^2)} \\ & + \frac{\mu_{43}\mu_{32}\mu_{21}}{\hbar^3} \frac{E_1 E_2 E_3^*}{(\Delta_{31} - \imath\Gamma_{31})(\Delta_{21} - \imath\Gamma_{21})} + \frac{\mu_{43}\mu_{34}\mu_{41}}{\hbar^3} \frac{|E_3|^2 E_4}{(\Delta_{31} - \imath\Gamma_{31})(\Delta_{41} - \imath\Gamma_{41})} \Bigg] e^{-\imath\omega_4 t}\end{aligned} \tag{31}$$

where Δ_{ij} represents the detuning between levels $|i\rangle$ and $|j\rangle$ and the corresponding photon, Γ_{ij} represents the decay rate of the corresponding coherence ρ_{ij} and γ_{ij} represents the decay of the population ρ_{ii}. Using the following definition of Rabi frequencies

$$\begin{aligned}\Omega_1 &= \mu_{12} E_1/\hbar \\ \Omega_2 &= \mu_{23} E_2/\hbar \\ \Omega_3 &= \mu_{34} E_3/\hbar \\ \Omega_4 &= \mu_{41} E_4/\hbar\end{aligned} \tag{32}$$

we rewrite Equations (30) and (31) in terms of these Rabi frequencies and solve numerically self consistently together with Maxwell's equations, Equations (16) and (17), for various values of z along the atomic ensemble and various values of detuning. The above approach is used for a different geometry of four-wave mixing by Boyd et al [14].

4.1. Results

The variation of the intensities of ω_3 and ω_4 photons as a function of distance along the sample for various detuning of pump 1 and pump 2 are shown in Figures 11 and 12. Figure 13 shows a colour intensity plot of the intensity of ω_3 for both values of detuning. In order to use Equations (30) and (31) it was necessary to start the calculations with very small values for Ω_3 and Ω_4.

From Figures 11 and 12 we can see an exponential growth in the intensities of the internally generated photons where the intensities depend heavily on the detuning of the lasers. The highest intensity occurs when both lasers have zero detuning. The intensity is also more sensitive to the detuning of the ω_1 laser.

5. Summary and Conclusion

We have investigated laser-atom interactions by first examining a two level atom interacting with a single laser beam where Rabi oscillations have been demonstrated. Dissipation effects show up as decay in the populations and de-coherence terms in the density matrix elements. Chaotic behaviour was also seen to occur when a modulated laser is used.

The analysis was extended to include saturated absorption spectroscopy and non-linear mixing processes in multi-level atoms. We showed that two additional coherent beams can be generated by four-wave mixing using two pump laser beams. The intensities of these beams depend on the detuning of the pump lasers.

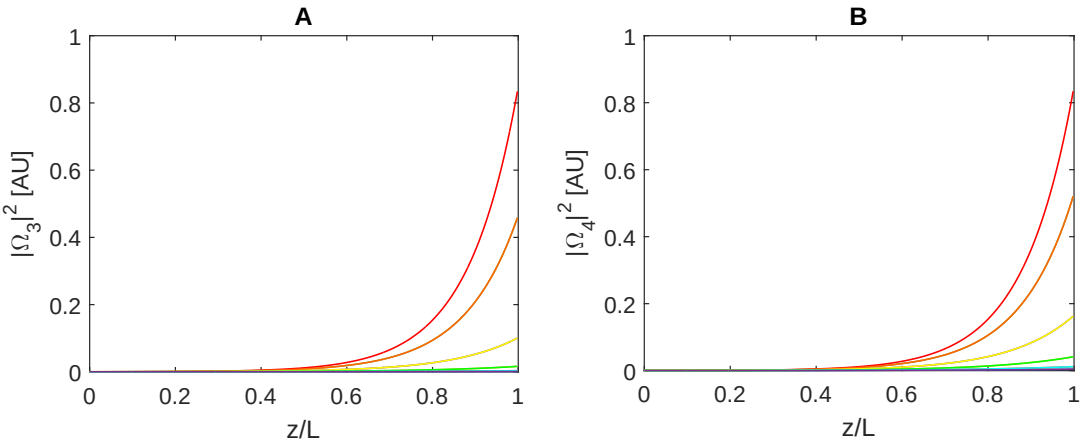

Figure 11. Intensities of the ω_3 (**A**) and ω_4 (**B**) photons for detuning values(Δ_{12}/Γ_{12}) (from top to bottom): 0 (red), 0.2 (orange), 0.4 (yellow), 0.6 (green), 0.8 (blue) and 1 (purple). These values are relative to the decoherence rate.

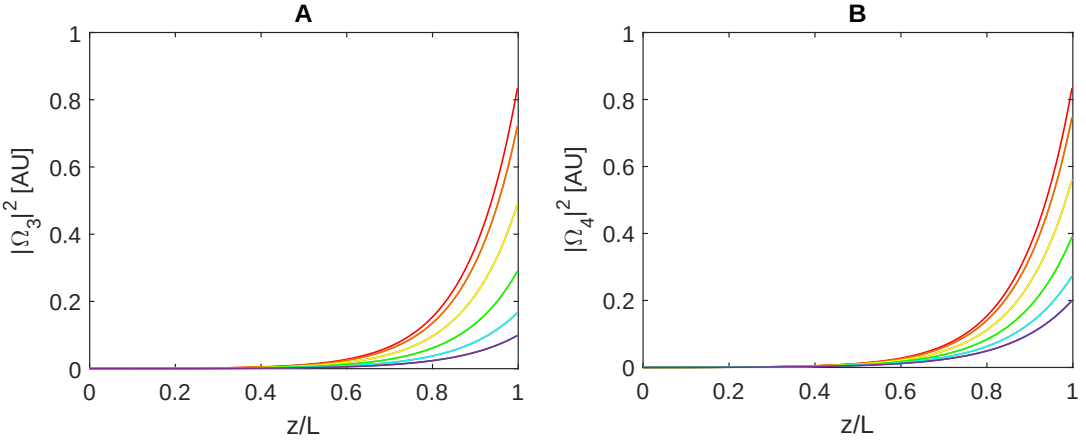

Figure 12. Intensities of the ω_3 (**A**) and ω_4 (**B**) photons for detuning values(Δ_{23}/Γ_{23}) (from top to bottom): 0 (red), 0.2 (orange), 0.4 (yellow), 0.6 (green), 0.8 (blue) and 1 (purple). These values are relative to the decoherence rate.

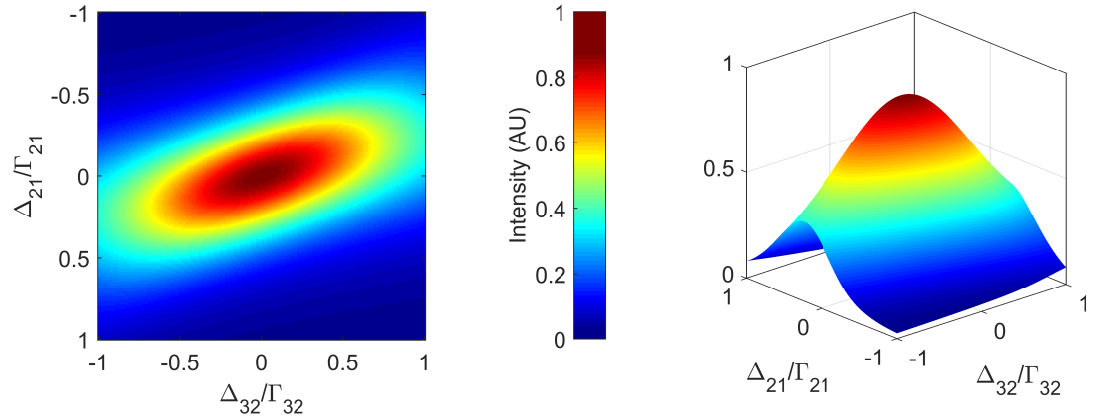

Figure 13. Colour plot of intensity of ω_3 photons as a function of detuning of pump 1 (Δ_{21}/Γ_{21}) and pump 2 (Δ_{32}/Γ_{32}).

References

[1] Allen L and Eberly J 1987 *Optical Resonance and Two-level Atoms* (New York: Dover)
[2] Grynberg G, Aspect A, Fabre C and Cohen-Tannoudji C 2010 *Introduction to Quantum Optics: From the Semi-classical Approach to Quantized Light* (Cambridge: Cambridge University Press)
[3] Loudon R 2000 *The Quantum Theory of Light* (Oxford: Oxford University Press)
[4] Jakowski J and Morokuma K 2009 *J. Chem. Phys.* **130** 224106
[5] Glushkov A V 2014 *JPCS* **548** 012020
[6] Glushkov A, Khetselius O Y, Svinarenko A A and Prepelitsa G P 2011 *Coherence and Ultrashort Pulse Laser Emission* (Croatia: Intech)
[7] Srivathsan B, Gulati G K, Brenda C M Y, Maslennikov G, Matsukevich D and Kurtsiefer C 2013 *Phys. Rev. Lett.* **111**(12) 123602
[8] de Melo N R and Vianna S S 2014 *J. Opt. Soc. Am. B* **31** 1735–1740
[9] Jen H H and Chen Y C 2016 *Phys. Rev. A* **93**(1) 013811
[10] Becerra F, Willis R, Rolston S and Orozco L 2011 *Rev. Mex. Fis.* **57** 23–28
[11] Vianna S S, Nussenzveig P, Magno W C and Tabosa J W R 1998 *Phys. Rev. A* **58**(4) 3000–3003
[12] Pisipati U, Almakrami I M, Joshi A and Serna J D 2012 *Am. J. Phys.* **80** 612–620
[13] Levenson M 1982 *Introduction to Nonlinear Laser Spectroscopy* (New York: Academic Press)
[14] Boyd R W, Malcuit M S, Gauthier D J and Rzążewski K 1987 *Phys. Rev. A* **35**(4) 1648–1658